processes

MDPI

Article

Energy Optimization through Heat and Power Integration on a Chlorobenzenes Production Plant

Nawaf S. Alqahtani, Turki A. Alrefai, Abdulaziz M. Almutlaq, Saeed M. Alzahrani and Ahmed E. Abasaeed *

Chemical Engineering Department, King Saud University, Riyadh 11421, Saudi Arabia; 439100630@student.ksu.edu.sa (N.S.A.); 439105376@student.ksu.edu.sa (T.A.A.); mutlaq@ksu.edu.sa (A.M.A.); szahrani@ksu.edu.sa (S.M.A.)

* Correspondence: abasaeed@ksu.edu.sa; Tel.: +966-507275840

Abstract: In this research work, an attempt has been made to address the heat and power integration opportunities for the process of the chlorination of benzene. This process produces a mixture of chlorobenzenes. To increase the production of the dichlorobenzene portion, the ratio of chlorine to benzene is typically 2:1. A process simulation model is designed using Aspen Plus for the production of 70,000 tons/year of dichlorobenzene via the reaction of liquid benzene with gaseous chlorine. Energy analysis is performed for the effective utilization of the utilities by networking the heat exchangers. This modification reduced the process heating and cooling requirements by 56.7% and 12.7%, respectively, and a reduction by 35.4% in the operating costs is achieved, while the annualized fixed cost increased by 9.6%; these changes resulted in savings in the total annual costs of about 10.9%.

Keywords: process integration; pinch analysis; monochlorobenzene; dichlorobenzene; benzene

check for updates

Citation: Alqahtani, N.S.; Alrefai, T.A.; Almutlaq, A.M.; Alzahrani, S.M.; Abasaeed, A.E. Energy Optimization through Heat and Power Integration on a Chlorobenzenes Production Plant. *Processes* **2024**, *12*, 569. https://doi.org/10.3390/pr12030569

Academic Editor: Shetian Liu

Received: 21 February 2024
Revised: 9 March 2024
Accepted: 11 March 2024
Published: 13 March 2024

Copyright: © 2024 by the authors. Licensee MDPI, Basel, Switzerland. This article is an open access article distributed under the terms and conditions of the Creative Commons Attribution (CC BY) license (https://creativecommons.org/licenses/by/4.0/).

1. Introduction

Chlorobenzenes are produced via the reaction of benzene with chlorine. This reaction is carried out in the presence of a catalyst such as ferric chloride, aluminum chloride, or stannic chloride. This process yields a mixture of chlorobenzene (CB), dichlorobenzene (DCB), and more chlorinated analogues. Controlled chlorination can be achieved by varying the ratio of chlorine to benzene in the feed. Dichlorobenzene has three isomeric forms, i.e., ortho-, para-, and meta-DCB. Although the demand for monochlorobenzene has been declining in agrochemical applications due to its carcinogenic nature and environmental issues, the demand for DCB is rapidly increasing. Nevertheless, chlorobenzene remains widely applicable in many fields such as rubber, plastics, pharmaceuticals, dyes, and pigments. On the other hand, dichlorobenzene is used as a precursor for the production of paints and coatings and has applications in electronics and agrochemicals industries [1]. Dorota et al. found that the solubility of N-alkylated naphthalene diimides (NDI) in dichlorobenzene or chloroform was highest for NDIC5-NDIC8, i.e., medium-length alkyl chains NDI which are used in electronics, photovoltaics, and sensors [2]. Huang and Shiau studied the effect of dichlorobenzene when used as an agrochemical on the stability of soil microbial communities. They showed that methanogens in oligotrophic soil can resist DCB; however, microorganisms such as *Pseudomonadaceae*, *Xanthomonadaceae*, and *Bacillales* can only resist DCB if abundant sources of nitrogen and phosphorous are available in the soil [3]. Han et al. improved ink-jetting properties by using a cosolvent composed of hexane and dichlorobenzene [4]. Many researchers have studied the removal of DCB. Ozerova et al. used carbon nanofibers (CNFs) containing chlorine and nitrogen to adsorb DCB from water. They determined that the addition of acetonitrile in the preparation of the CNF increased its adsorption capacity by 28%. CNFs were capable of adsorbing over 90% of DCB from water. The hydrodechlorination of CNF doped with palladium nanoparticles resulted in the complete removal of DCB from CNFs [5]. Jurkiewicz and Pełech showed that modified carbon nanotubes (CNT) and activated carbon (AC) are effective adsorbents

in the removal of DCB from the aqueous phase. Activated carbon outperformed the CNT in terms of DCB recovery and regeneration. DCB recovery was in the range of 76–85% for AC compared to 23–46% for CNT [6].

Generally speaking, mass and/or heat integration are performed to fully utilize the available resources, being material or energy, within a plant so as to minimize or eliminate the need for external resources or waste generation, thus leading to improved plant economics [7,8]. Pinch technology is commonly used to integrate heat within a unit, e.g., distillation columns, or the whole plant, or to retrofit existing heat exchanger networks [9–13]. The main rules in applying pinch technology require the observation that no external cooling is performed above the pinch, whereas below the pinch, there is no external heating, and heat does not transfer across the pinch. Alkhathiri et al. applied pinch technology to optimize heat requirements in a plant that produces ethylene through the oxidative coupling of methane. They showed that the heating utility was reduced by 90%, whereas the cooling utility was reduced by more than 60% [10]. Nemet et al. applied pinch analysis to integrate an absorber chiller that uses heat instead of electricity with a process. By placing the absorption chiller below the pinch, they were able to completely reduce the consumption of the hot utility [11]. Ulyev et al. applied heat integration on an industrial plant that produces ethylbenzene by reacting ethylene with benzene. They retrofitted four heat exchanger networks and determined a reduction of 34% for both steam consumption and carbon dioxide emissions for the best one [14]. López-Fernández et al. designed and applied pinch analysis on a system that produces biojet fuel from plastic wastes and biomass that uses gasification and Fischer–Tropsch processes. They reported a reduction in heating and cooling demands by 100% and 41.6%, respectively [15]. Puhar et al. applied pinch analysis on the production of formalin via the steam reforming of methane. They determined that heat integration resulted in reducing the heat consumption by 39%, the capital cost by 11%, and the environmental footprint by 7–22% [16]. Wang et al. [17] applied exergy and pinch analyses to optimize a combined cycle power plant. They reported an overall energy efficiency increase of 70.56% after optimization compared to 68.73% before, as well as a 5.56% reduction in exergy losses in the high-pressure section.

In this contribution, a process for the production of 70,000 tons/year of chlorobenzenes through the chlorination of benzene is developed. Power and heat integration are performed to optimize the energy requirements of the plant. Aspen Plus V14 process simulation software is used to perform the necessary calculations and the energy analyzer is used to achieve the most efficient utilization of the utilities.

2. Process Flowsheet

The chlorination of benzene is an electrophilic substitution process with Cl^+ as the electrophile. The reaction takes place in the presence of a Lewis acid catalyst. Chlorobenzenes are prepared industrially by the reaction of liquid benzene with gaseous chlorine in the presence of a catalyst at moderate temperature and atmospheric pressure. Hydrogen chloride is formed as a by-product. Generally, mixtures of isomers and compounds with varying degrees of chlorination are obtained because any given chlorobenzene can be further chlorinated up to the stage of hexachlorobenzene. Mainly, the degree of chlorination depends on the chlorine-to-benzene molar ratio. Franck and Stadelhofer [18] reported the formation of polychlorinated benzenes in relation to the chlorine-to-benzene molar ratio in a batch chlorination, chlorination in continuous stirred tank reactors, and in a two-cascade reactor at a reaction temperature of 55 °C and using ferric chloride as the catalyst. From their findings and since the desired product is dichlorobenzene, a molar ratio of chlorine to benzene of 2:1 will give a 3:1 dichlorobenzene-to-monochlorobenzene molar ratio. The reaction is usually conducted in an isothermal continuous stirred tank reactor at a temperature of 55 °C and using ferric chloride as the catalyst.

2.1. Production of Chlorobenzenes

Figure 1 shows the process flowsheet before heat integration. The stream number is written inside a rhombus shape on the lines, whereas the process and its units are described below. Liquid benzene and chlorine gas are fed to the process, via two separate streams, at a temperature of 25 °C and a pressure of 1 atm. The liquid benzene is pumped (P-101) and chlorine gas passes through a compressor (C-101) at 2.4 bar. The pump is assumed to be operating isothermally; however, as a result of the pressure increase, the chlorine gas leaves the compressor at a temperature of 95.59 °C. The liquid benzene and chlorine gas feed streams, after being pressurized, are mixed with the recycle streams in an adiabatic mixer (M-101). The mixed streams leave the mixer at a temperature of 53.06 °C before they enter a heat exchanger where they are heated to 55 °C, which is the optimal temperature of the chlorination reactor (R-101). The heated stream (#6) enters a catalyzed continuously stirred tank reactor. The reactor (R-101) operates isothermally at 55 °C. The mixed liquid–gas phase reaction is exothermic; therefore, cooling is required to keep the desired reactor temperature constant. The effluent from the reactor (R-101) at 55 °C is cooled to 35 °C in a heat exchanger (E-102). This is the most optimal operating temperature for the flash separator as it provides the best possible separation at an operating pressure of 2.4 bar.

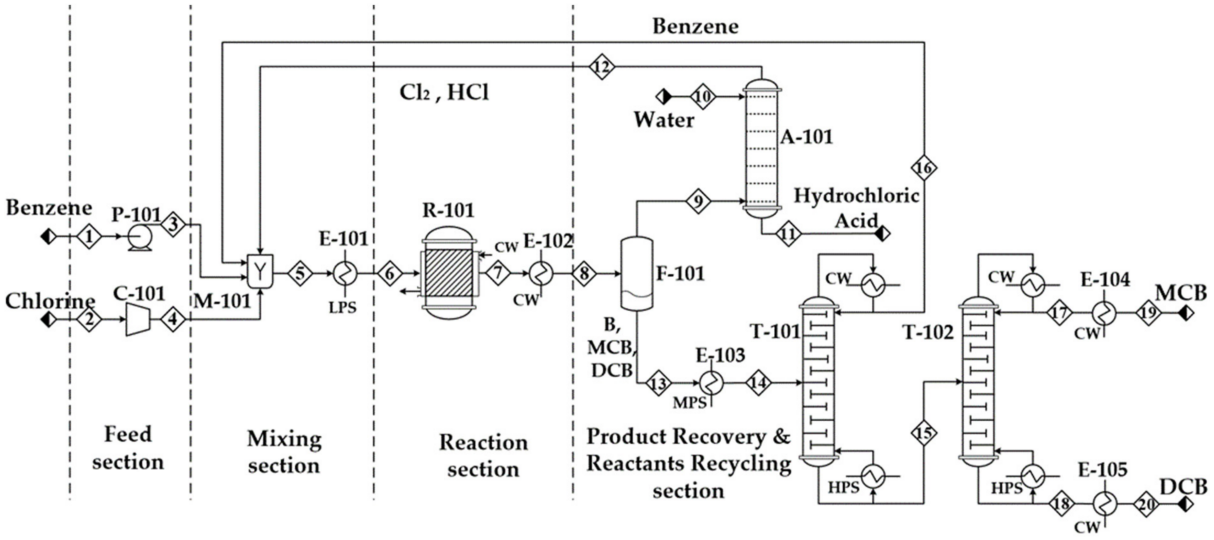


Figure 1. Process flowsheet.

2.2. Products Recovery and Reactants Recycling

The cooled stream (#8) is then fed to an isothermal flash drum (F-101) operated at 35 °C and 2.4 bar. The liquid product stream (#13) contains mostly benzene, monochlorobenzene, and dichlorobenzene, while chlorine and hydrogen chloride exit the flash drum in the vapor stream (#9). Stream #13 leaving the flash drum (F-101) at 35 °C is heated to 140 °C, which is the optimal feed temperature of the first distillation tower (T-101). The stream leaving the top of the tower consisting of 99.99% of the benzene fed, along with the chlorine and hydrogen chloride traces, is sent to the mixer (M-101) at 96.34 °C as a recycle stream. Meanwhile, the bottom stream, which consists of 99.99% of the fed monochlorobenzene, the dichlorobenzene, and traces of benzene, is fed to a second distillation tower (T-102) at 200.46 °C. The tower (T-102) recovers 99% of the fed monochlorobenzene and dichlorobenzene in the top and bottom streams, respectively. The top stream leaves at 166.9 °C, while the bottom stream leaves at a temperature of 219.18 °C. The benzene traces leave the tower along with the monochlorobenzene in the top stream.

The flash drums (F-101) vapor effluent, containing mostly hydrogen chloride and chlorine at 35 °C and 2.4 bar, is fed to the bottom of an isothermal absorption tower (A-101). Pure water is fed to the top of the tower at 35 °C and 2.4 bar as well. The tower produces a bottom stream containing all the water and hydrogen chloride fed, along with all the

benzene, monochlorobenzene, and dichlorobenzene traces. Meanwhile, the fed chlorine gas leaves the top of the tower at 35 °C and is sent to the mixer (M-101) as a recycle stream.

3. Process Pinch Analysis Methodology

Process heat integration is an essential aspect for enhancing industrial energy efficiency and minimizing environmental impact. Engineers are able to identify opportunities for maximizing the utilization of energy streams inside a process using pinch analysis techniques. Additionally, process heat integration mitigates operational expenses by reducing energy consumption. It also mitigates greenhouse gas emissions by reducing the demand for extra energy to be generated off-site. Process heat integration will become increasingly critical for manufacturing industries attempting to reduce their energy use and carbon footprint through novel thermal integration technologies as resources become more restrictive and environmentally conscious regulations are introduced.

3.1. Data Extraction

The first step is to identify the process streams that can be included in the process heat integration. The selected streams fall into two categories: cold streams that need to be heated or can be used for cooling other streams, and hot streams that need to be cooled or can be used for heating other streams.

From the material and energy balance calculations, the stream data can be extracted; the required data are the temperature range (supplied and target temperatures), the stream category (hot or cold), and the stream heat capacity flow rate CP (kW/K) or the stream heat load ΔH (kW); their values are given in Tables 1 and 2. Stream #7 is excluded because of the equal heating and cooling duties as shown in the tables and also to avoid a threshold problem.

$$\Delta H = CP\,\Delta T \tag{1}$$

$$CP = \dot{m} C_p \tag{2}$$

where $\dot{m}$ = mass flow rate (kg/s) and C_p = specific heat capacity (kJ·kg^{-1}K^{-1}).

Table 1. Cold streams data.

Stream	Supplied Temperature, °C	Targeted Temperature, °C	*CP*, kW/K	Δ*H*, kW
3	25	55	3.296	98.9
12	35	55	0.621	12.4
13	35	140	5.288	555.2

Table 2. Hot streams data.

Stream	Supplied Temperature, °C	Targeted Temperature, °C	*CP*, kW/K	Δ*H*, kW
4	95.6	55	1.354	−94.97
16	96.3	55	1.064	−43.95
17	166.9	35	0.913	−120.42
18	160	35	3.342	−417.75

3.2. Choosing ΔT_{min}

In pinch analysis, the importance of ΔT_{min} (the minimum allowed temperature difference) is critical and must be optimized based on the tradeoff between the capital and operating cost; the optimal ΔT_{min} (10 °C) is taken (a typical value for petrochemical plants is around 10 °C [8]). The shifted composite curve is, then, used to calculate energy targets and pinch temperature. the process streams temperatures are divided into intervals based on the supply and target temperature of each stream, then total enthalpy of each interval is calculated for the hot and cold composites separately.

To determine the pinch temperature, ΔT_{min} is divided by two; then, the result (5 °C) is subtracted from the hot streams temperatures and added to the cold streams value. Based on Figure 2, the pinch temperature is 40 °C. Therefore, the cold and hot streams' pinch temperatures are listed in Table 3.

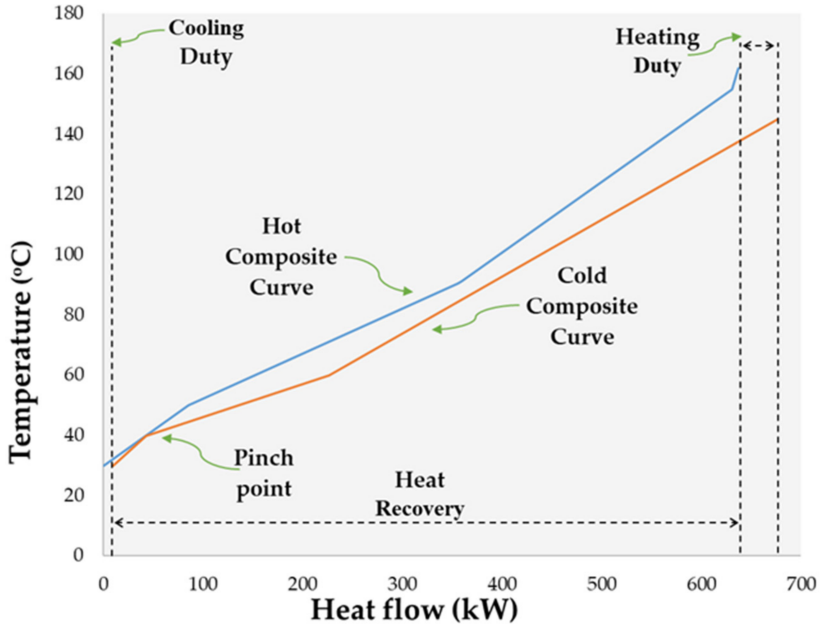


Figure 2. Process shifted composite curve.

Table 3. Cold and hot streams pinch temperatures.

Streams	Pinch Temperatures
Cold Streams	35 °C
Hot Streams	45 °C

The cooling and heating energy targets are obtained from the process shifted composite curve (Figure 2) and are listed in Table 4.

Table 4. Energy targets.

Energy Targets	kW
Cooling Target	9.6
Heating Target	39.0
Recovery Target	627.5

Figure 3 shows the grand composite curve (GCC) for the process. It shows the effect of heat integration on lowering the utilities' demand to lower grades than the original process due to matching the surplus heat to the deficit one.

3.3. Heat Exchanger Network Design

To achieve the energy targets, a heat exchanger network (HEN) should be carried out. This is called MER design, which stands for the maximum energy recovery or minimum energy requirement. To achieve minimum utility targets, there are three golden rules that should be followed; i.e., heat should not be transferred across the pinch, cold utilities are not used above the pinch, and hot utilities are not used below the pinch [19–21].

To design the heat exchanger network, the grid diagram will be used [20]. The problem here is split into two subproblems, one above the pinch and the other below it, as shown in Figure 4.

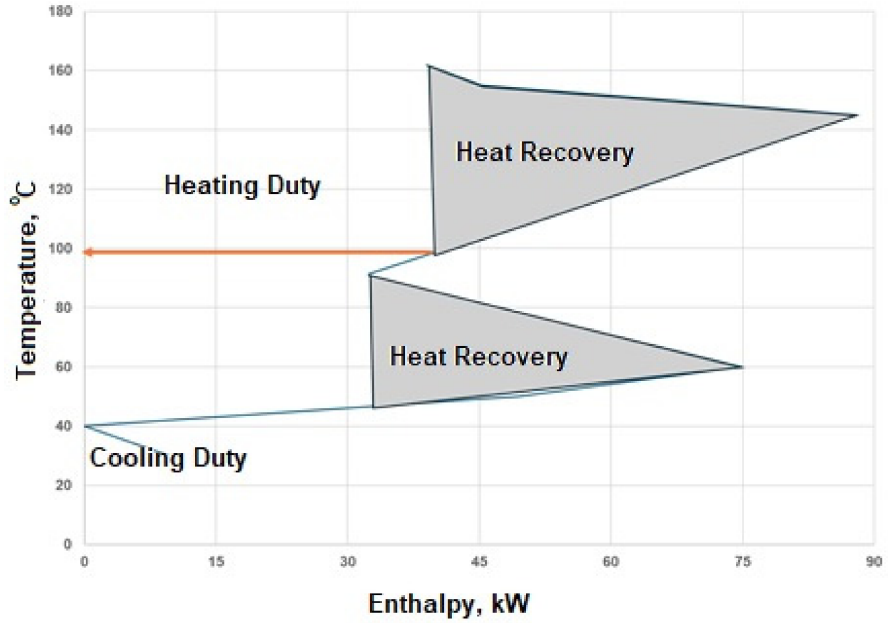


Figure 3. Grand composite curve for the process.

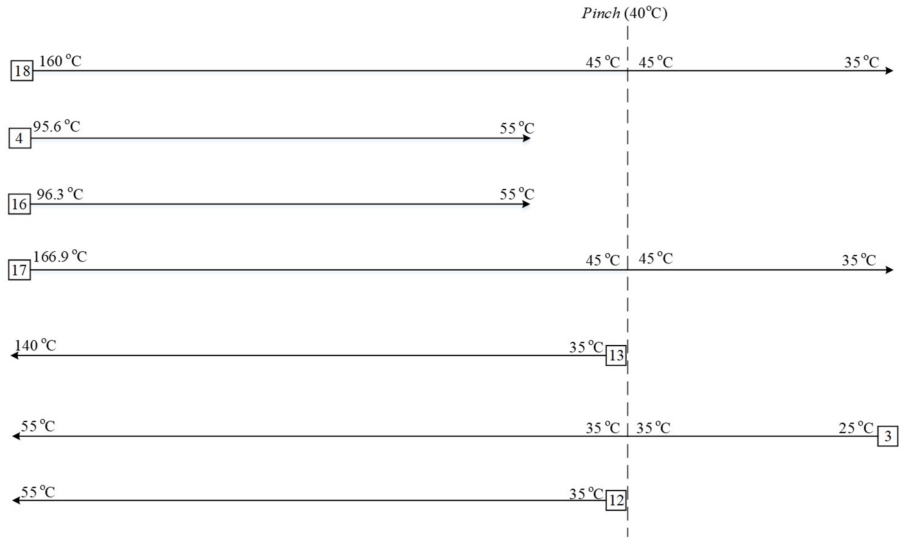


Figure 4. Process grid diagram.

The matching of heat exchangers has rules and guidelines [19–21] based on the stream population and the heat capacity of each stream. It is worth mentioning that the minimum number of heat exchangers can be determined ahead of the detailed design.

Based on the data that have been extracted and the energy targets, and by following the heat exchanger network design criteria, the following heat exchanger network was constructed above and below the pinch; the heat exchanger network designs are shown in Figures 5 and 6.

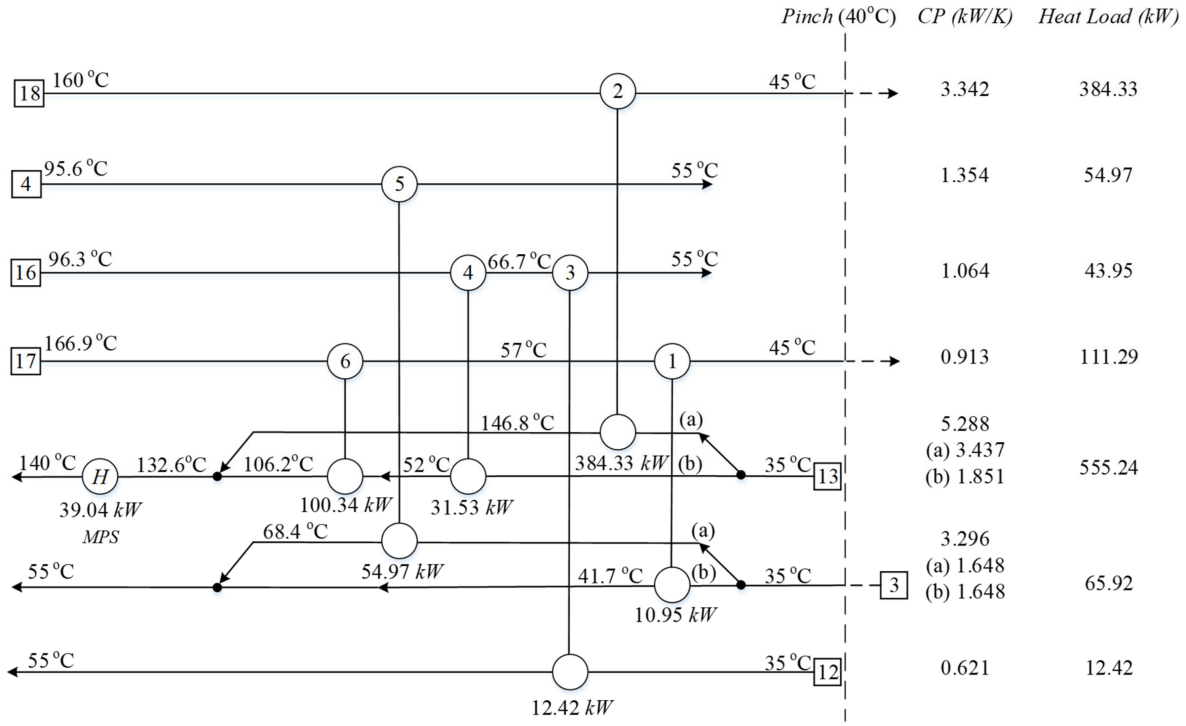


Figure 5. Network design above pinch.

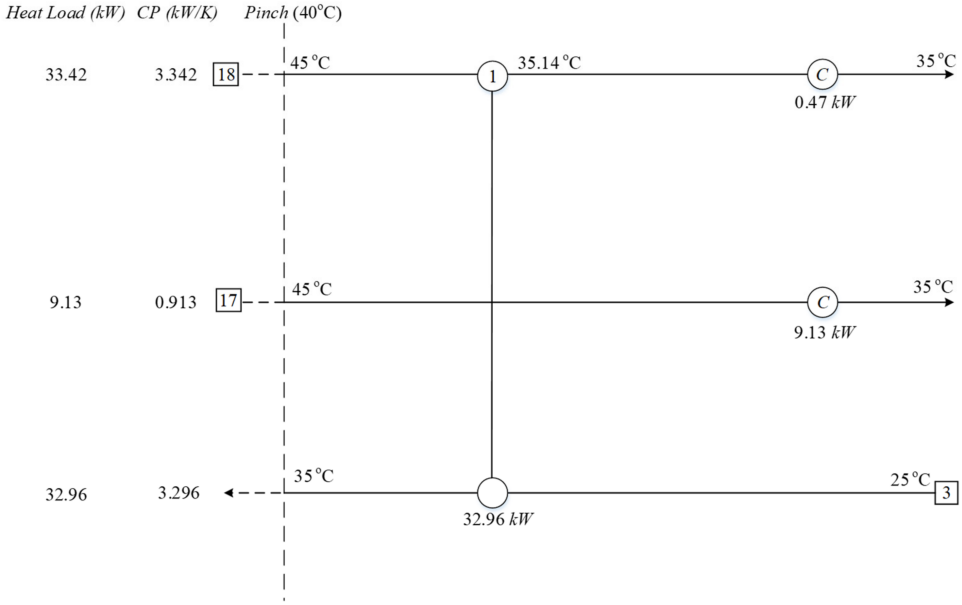


Figure 6. Network design below pinch.

3.4. Network Relaxation

Dividing the heat exchanger network design into two regions above and below the pinch will result in increasing the number of minimum number of units. So, eliminating small heat exchangers and dividing the load among the other heat exchangers is often beneficial, due to the reduction in the fixed capital investment caused by the reduction in the number of units, which also simplifies the network.

The minimum number of units can be calculated by using the following equation [19]:

$$u_{min} = N - 1 \quad (3)$$

where

u = number of units (including heaters and coolers);
N = number of streams (including utilities);
$u_{min,\ above\ pinch}$ = 4 hot streams + 3 cold streams + 1 heating utility − 1 = 7 units;
$u_{min,\ below\ pinch}$ = 2 hot streams + 1 cold streams + 1 cooling utility − 1 = 3 units;
$u_{min,\ before\ dividing}$ = 4 hot streams + 3 cold streams + 1 heating utility + 1 cooling utility − 1 = 8 units.

The number of units achieved by the network design is 7 units above the pinch and 3 units below the pinch for a total of 10 units, which is more than 8 units. To achieve the minimum number of units, the loops across the pinch and paths in the system must be recognized, breaking the loops by subtracting and adding loads, and modifying the paths.

As shown in Figure 7, in the network, there is one loop that can be eliminated, starting with the cooler at stream #18 passing through heat exchangers (#1, #2, and #7), ending with the heater, that can be broken by eliminating heat exchanger (#1) and adding the load to the cooler, heater, and heat exchanger (#2), and subtracting that load from heat exchanger (#7).

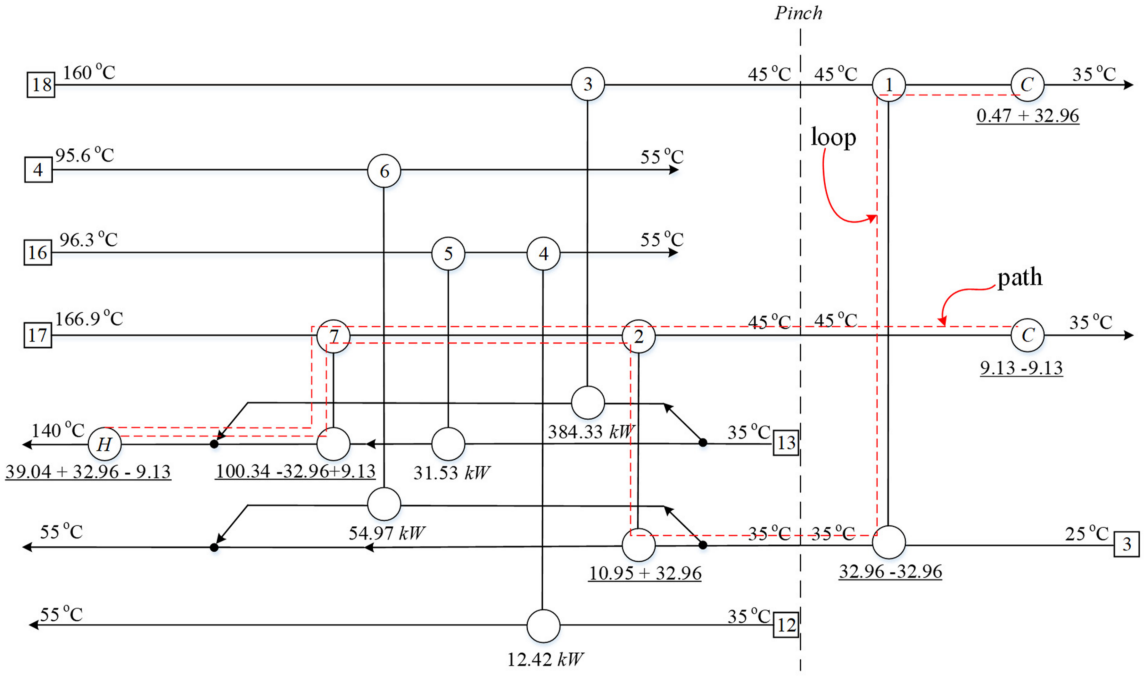


Figure 7. Relaxed network.

Additionally, there is path to eliminate the stream #17 cooler since it has the smallest load, starting with the cooler at stream #17 passing through heat exchangers (#2) and (#7), ending with the heater, by adding the load to heat exchanger (#7) and subtracting that load from the heater or the cooler that has been eliminated. As shown in Figure 7, the u_{min} has been achieved.

Figure 8 shows the network design after eliminating the two heat exchangers and recalculating the loads, as well as the minimum number of units.

3.5. Heat and Power

Heat integration can be taken one step further by incorporating heat and power integration to the distillation units shown in Figure 9; there is a very strong potential to reduce the heat loads of the distillation columns through open cycle mechanical vapor recompression (MVR) [7]. This is conducted by elevating the overhead stream temperature above that of the bottom stream while keeping the minimum approach temperature.

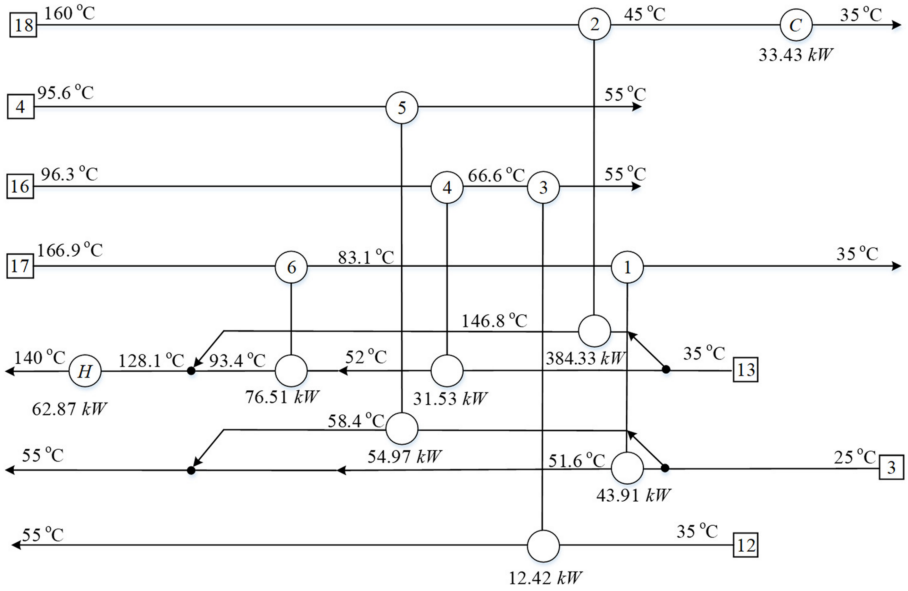


Figure 8. Process heat exchanger network.

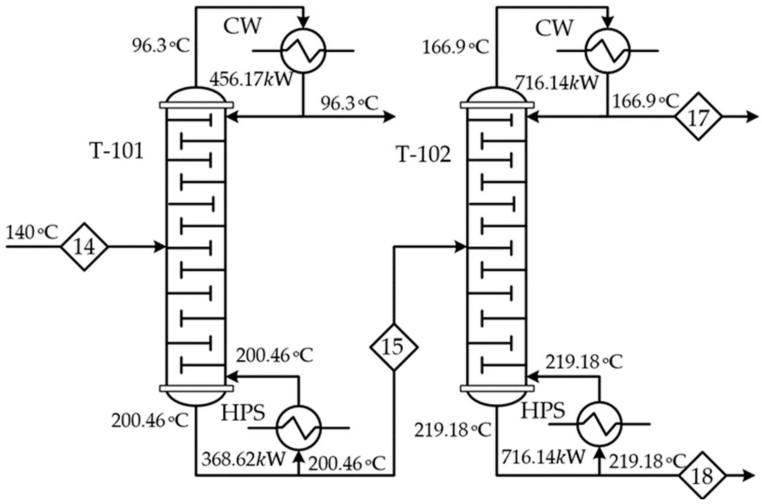


Figure 9. Process distillation columns.

Integrating the (T-102) overhead stream with the (T-101) bottom stream is investigated. For a 10 °C temperature driving force, and since the (T-101) bottom stream bubble point temperature is 200.46 °C, the overhead stream temperature from (T-102) should be elevated to 210.46 °C. Based on that, the calculations have been performed based on only latent heat exchange, where the overhead mass flow rate is 2.2542 kg/s. To calculate the required flow rate for the (T-101) reboiler, the overhead stream latent heat is needed, which is 272.56 kJ/kg at 5.75 bar. The mass flow rate of the heating fluid can be calculated by using the following equation:

$$\dot{m} = \frac{Q_R}{\lambda} = \frac{368.62}{272.56} = 1.3525 \text{ kg/s} \quad (4)$$

where $\dot{m}$ = mass flow rate (kg/s); Q_R = reboiler duty (kJ/s); and λ = overhead stream latent heat (kJ/kg).

Therefore, the overhead stream will be split into two fractions with the ratios shown in Figure 10. The overhead saturated vapor is passed through a throttling valve to reduce its pressure to 1.01 bar to prevent cavitation problems, then the stream is fed to compressor where it is pressurized to the desired pressure of 5.75 bar. The compressor outlet

stream temperature and the required compression power are calculated via the following equations [7]:

$$\frac{T_{out}}{T_{in}} = \left(\frac{P_{out}}{P_{in}}\right)^{\left(\frac{\gamma-1}{\gamma}\right)} \tag{5}$$

$$W = \dot{m}\left(\frac{\gamma}{\gamma-1}\right)\left(\frac{R}{Mw \times \eta_{isentropic}}\right)(T_{out} - T_{in}) \tag{6}$$

where T (K); P (bar); $\dot{m}$ (kg/s); $\gamma = C_P/C_v = 1.075$; $\eta_{isentropic}$ = isentropic efficiency of the compressor, assumed to be 90%; and Mw = molecular weight of the overhead vapor, 112.9 kg/kmol.

$$T_{out} = 443.05\left(\frac{5.75}{1.01}\right)^{\left(\frac{1.075-1}{1.075}\right)} = 500.2\ K = 227.05\ ^{\circ}\text{C}$$

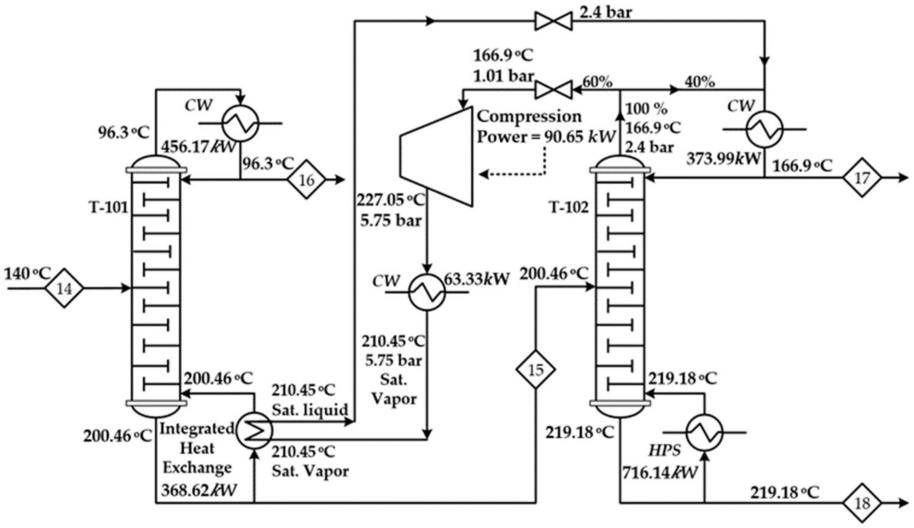


Figure 10. Mechanical vapor recompression (MVR) system.

To cool this stream to 210.46 °C, 63.33 kW of cooling water will be needed.

$$Compression\ Power = 1.3525\left(\frac{1.075}{1.075-1}\right)\left(\frac{8.314}{112.903 \times 0.9}\right)(500.2 - 443.05) = 90.65\ \text{kW}$$

The compressed portion of column (T-102) overhead is then cooled to the desired temperature and then sent to the (T-101) reboiler as a heating media. Because of that, the high-pressure steam (HPS) is no longer needed and the heat will be provided from the (T-102) overhead vapor; also, the cooling water of the (T-102) condenser will be reduced to almost half, as illustrated in Figure 10.

3.6. Results of Combining MVR System with HEN

Since the compressed overhead vapor needs cooling duties of 63.3 kW and the HEN heating requirement is 62.87 kW, and the temperature driving force is high in heat exchanger, the load will be 63.33 kW, which is more than the HEN heating requirements by 0.46 kW. This will result in an increase in the outlet temperature of stream #13 from 140 °C to 140.08 °C, which will not affect (T-101) operation. The cooling and heating requirements and one heat exchanger have been eliminated. The integrated process flow sheet is shown in Figure 11.

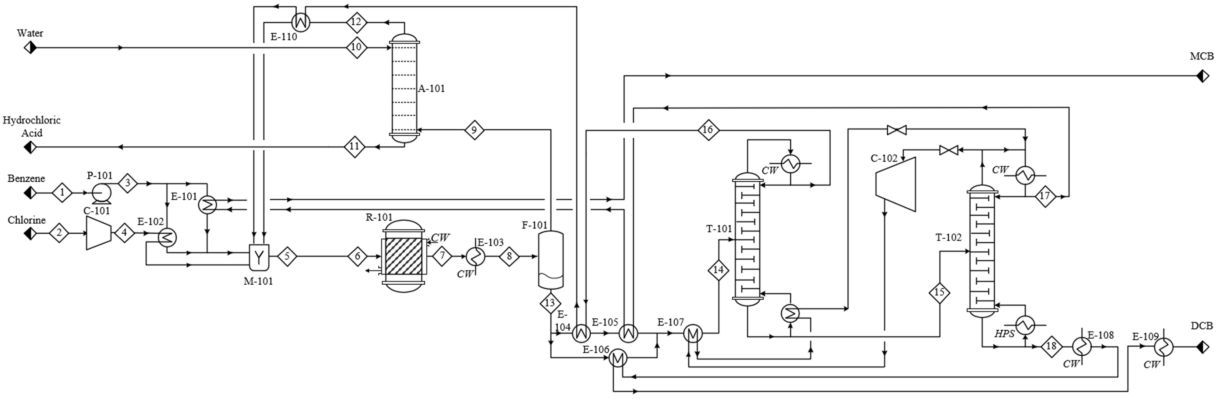


Figure 11. Integrated process flow sheet.

Finally, after conducting the pinch analysis and combining the MVR system with HEN, the energy requirements for the process is reduced by 21.2%, as listed in Table 5. The reduction in operating cost will be more than 21.2%, since the reduction in the heating requirements is 56.7% and heating utilities are more expensive than cooling utilities, as will be illustrated in the economic study.

Table 5. Energy requirements savings.

Energy Requirements (kW)	Non-Integrated	Integrated	Savings
Cooling	6936.2	6053.1	12.7%
Heating	1652.0	716.1	56.7%
Overall	8588.2	6769.3	21.2%

4. Economic Study for Non-Integrated and Integrated Process

As mentioned previously, the reduction in operating costs will be more than 21.2% because the reduction in the heating requirements is 56.7%. Taking the increase in fixed capital investment into account, the savings from heat integration will be illustrated to identify the feasibility of the heat integration.

4.1. Impact of the Network Relaxation on the Total Annualized Cost

To demonstrate the benefit of the network relaxation, the operating and fixed costs before and after relaxation are presented in Table 6.

Table 6. Operating and fixed cost before and after relaxation.

	Cost $/Year	
	Before	**After**
Operating Cost	5996	9870
Annualized Fixed Cost	73,147	61,479
Annualized Total Cost	79,143	71,349

4.2. Impact of Process Heat Integration on Fixed and Operating Costs

Utilities used in this process along with their costs are tabulated in Table 7. The overall annual utility cost based on the utility demand of each equipment in the integrated and non-integrated process is calculated and tabulated in Table 8.

Table 7. Costs of utilities used [22].

Utility Type	Cost
Cooling Water	15.7 \$/1000 m^3
High Pressure Steam	9.61 \$/1000 kg
Medium Pressure Steam	9.54 \$/1000 kg
Low Pressure Steam	9.45 \$/1000 kg
Electricity	0.0674 \$/kWh

Table 8. Overall annual utility cost.

Equipment	Utility Demand	Utility Type	Utility Cost (\$ per Year)	
			Non-Integrated	Integrated
(E-101)	20.11 kg/h eliminated in the integrated process	LPS	1505	0
(E-102)	3.35 kg/s	Cooling Water	1497	1497
(E-103)	1306.74 kg/h	MPS	98,732	0
(E-104)	2.95 kg/s	Cooling Water	1318	0
(E-105)	15.17 kg/s reduced to 5.2 kg/s in the integrated process	Cooling Water	6791	2325
(T-101) Reboiler	781.47 kg/h eliminated in the integrated process	HPS	59,478	0
(T-101) Condenser	7.27 kg/s	Cooling Water	3256	3256
(T-102) Reboiler	1518.21 kg/h	HPS	115,552	115,552
(T-102) Condenser	11.41 kg/s reduced to 5.96 kg/s in the integrated process	Cooling Water	5108	2667
(R-101) Cooling Jacket	58.19 kg/s	Cooling Water	26,048	26,048
(C-101)	0.56 kW	Electricity	299	299
(P-101)	33.25 kW	Electricity	17,775	17,775
(C-102)	90.65 kW added in the integrated process	Electricity	0	48,461
Overall Annual Utility Cost			337,364	217,884

As a result of the process heat integration, the system has a reduction in the operating costs by USD 119,480, which corresponds to a 35.4% reduction in the operating costs. Keeping in mind that the economic feasibility is sensitive to changes in fixed capital investment, the annualized fixed capital investment is calculated based on an annual interest rate of 5%, which is higher than average annual interest rate for petrochemical plants. The following equation will be used to calculate the required fixed capital investment (FCI) to construct HEN and the MVR system.

$$FCI = (FCC_{HEN} + FCC_{MVR}) - FCE_{HE} \tag{7}$$

$$FCI = (1,097,200 + 514,664) - 716,000 = 895,864 \text{ USD}$$

where FCC_{HEN} = fixed cost of constructing HEN; FCC_{MVR} = fixed cost of constructing MVR; and FCE_{HE} = fixed cost of eliminating heat exchangers.

The annualized fixed cost (AFC) is calculated using the following equation [7]:

$$AFC = FCI \times \left(\frac{i(1+i)^N}{(1+i)^N - 1} \right) \tag{8}$$

where N = project lifetime (15 years) and i = annual interest rate.

$$AFC = 895,864 \times \left(\frac{0.05(1+0.05)^{15}}{(1+0.05)^{15}-1}\right)\left(\frac{0.05\ (1+0.05)^{15}}{(1+0.05)\ ^{15}-1}\right) = 86,310 \text{ USD}$$

5. Conclusions

A process flowsheet for the production of monochlorobenzene and dichlorobenzene through the chlorination of benzene was simulated by Aspen Plus. In order to favor the production of dichlorobenzene over chlorobenzene, the reactor feed ratio of chlorine to benzene was kept at 2:1. Heat and power integration showed that it is possible to save about 56.7% and 12.7% on the heating and cooling requirements. The economic evaluation of the integrated process revealed a reduction in the operating cost by 35.4%, while the annualized fixed cost increased by 9.6%. Overall, the savings in total annual costs was about 10.9%.

Author Contributions: Conceptualization, S.M.A. and A.E.A.; methodology, N.S.A., T.A.A., A.M.A., S.M.A. and A.E.A.; software, N.S.A., T.A.A. and A.M.A.; validation, N.S.A., T.A.A. and A.M.A.; formal analysis, N.S.A., T.A.A., A.M.A. and A.E.A.; investigation, N.S.A., T.A.A. and A.M.A.; resources, A.M.A., S.M.A. and A.E.A.; data curation, N.S.A. and A.M.A.; writing—original draft preparation, N.S.A., T.A.A., A.M.A. and A.E.A.; writing—review and editing, N.S.A., A.M.A., S.M.A. and A.E.A.; visualization, S.M.A. and A.E.A.; supervision, A.E.A.; project administration, S.M.A. and A.E.A.; funding acquisition, S.M.A. All authors have read and agreed to the published version of the manuscript.

Funding: The authors are very grateful to SABIC Polymer Research Center (SPRC) at the Chemical Engineering Department, King Saud University, for funding the project.

Data Availability Statement: Data are contained within the article.

Conflicts of Interest: The authors declare no conflicts of interest.

References

1. Yoshio, N.; Biegler, L.T. Demand-Based Optimization of a Chlorobenzene Process with High-Fidelity and Surrogate Reactor Models Under Trust Region Strategies. *AIChE J.* **2021**, *67*, e17054. [CrossRef]
2. Chlebosz, D.; Goldeman, W.; Janus, K.; Szuster, M.; Kiersnowski, A. Synthesis, Solution, and Solid-State Properties of Homological Dialkylated Naphthalene Diimides—A Systematic Review of Molecules for Next-Generation Organic Electronics. *Molecules* **2023**, *28*, 2940. [CrossRef] [PubMed]
3. Huang, W.T.; Shiau, Y.J. Potential Changes in Soil Microbial Composition under 1,2-Dichlorobenzene Contamination. *Sustainability* **2023**, *15*, 1432. [CrossRef]
4. Han, Y.J.; Kim, D.Y.; An, K.; Kang, K.T.; Ju, B.K.; Cho, K.H. sequential Improvement from Cosolvents Ink Formulation to Vacuum Annealing for Ink-Jet Printed Quantum-Dot Light-Emitting Diodes. *Materials* **2020**, *13*, 4754. [CrossRef] [PubMed]
5. Ozerova, A.M.; Potylitsyna, A.R.; Bauman, Y.I.; Tayban, E.S.; Lipatnikova, I.L.; Nartova, A.V.; Vedyagin, A.A.; Mishakov, I.V.; Shubin, Y.V.; Netskina, O.V. Synthesis of Chlorine- and Nitrogen-Containing Carbon Nanofibers for Water Purification from Chloroaromatic Compounds. *Materials* **2022**, *15*, 8414. [CrossRef] [PubMed]
6. Jurkiewicz, M.; Pełech, R. Adsorption of 1,2-Dichlorobenzene from the Aqueous Phase onto Activated Carbons and Modified Carbon Nanotubes. *Int. J. Mol. Sci.* **2021**, *22*, 13152. [CrossRef] [PubMed]
7. El-Halwagi, M.M. *Sustainable Design through Process Integration*; Elsevier Science: Amsterdam, The Netherlands, 2017.
8. Kemp, I.C. *Pinch Analysis and Process Integration, a User Guide on Process Integration for the Efficient Use of Energy*, 2nd ed.; Butterworth-Heinemann: Oxford, UK, 2007.
9. Linnhoff, B.; Dunford, H.; Smith, R. Heat integration of distillation columns into overall processes. *Chem. Eng. Sci.* **1983**, *38*, 1175. [CrossRef]
10. Alkathiri, R.; Alshamrani, A.; Wazeer, I.; Boumaza, M.; Haj-Kali, M.K. Optimization of the Oxidative Coupling of Methane Process for Ethylene Production. *Processes* **2022**, *10*, 1085. [CrossRef]
11. Nemet, A.; Kravanja, Z.; Bogataj, M. Integration of an Absorption Chiller to a Process Applying the Pinch Analysis Approach. *Processes* **2022**, *10*, 1028. [CrossRef]
12. Walden, J.V.M.; Wellig, B.; Stathopoulos, P. Heat pump integration in non-continuous industrial processes by Dynamic Pinch Analysis Targeting. *Appl. Energy* **2023**, *352*, 121933. [CrossRef]
13. Berchiche, A.; Guenoune, M.; Belaadi, S.; Léonard, G. Optimal Energy Integration and Off-Design Analysis of an Amine-Based Natural Gas Sweetening Unit. *Appl. Sci.* **2023**, *13*, 6559. [CrossRef]

14. Ulyev, L.M.; Kanischev, M.V.; Chibisov, R.E.; Vasilyev, M.A. Heat Integration of an Industrial Unit for the Ethylbenzene Production. *Energies* **2021**, *10*, 3839. [CrossRef]
15. López-Fernández, A.; Bolonio, D.; Amez, I.; Castells, B.; Ortega, M.F.; García-Martínez, M.J. Design and Pinch Analysis of a GFT Process for Production of Biojet Fuel from Biomass and Plastics. *Energies* **2021**, *14*, 6035. [CrossRef]
16. Puhar, J.; Vujanović, A.; Awad, P.; Čuček, L. Reduction of Cost, Energy and Emissions of the Formalin Production Process via Methane Steam Reforming. *Systems* **2021**, *9*, 5. [CrossRef]
17. Wang, D.; Zou, Y.; Farjam, H. Analysis and Optimization of Thermal Power Plants: Pinch and Exergy Methods. *J. Clean. Prod.* **2023**, *430*, 139287. [CrossRef]
18. Franck, H.G.; Stadelhofer, J.W. *Industrial Aromatic Chemistry Raw Materials·Processes·Products*; Illustrated Edition; Springer: Berlin/Heidelberg, Germany, 1988.
19. Linnhoff, B.; Flower, J.R. Synthesis of heat exchanger networks: Part I: Systematic generation of energy optimal networks. *AIChE J.* **1978**, *24*, 633. [CrossRef]
20. Linnhoff, B.; Flower, J.R. Synthesis of heat exchanger networks: Part II: Evolutionary generation of networks with various criteria of optimality. *AIChE J.* **1978**, *24*, 642. [CrossRef]
21. Linnhoff, B.; Hindmarsh, E. The pinch design method of heat exchanger networks. *Chem. Eng. Sci.* **1983**, *38*, 745. [CrossRef]
22. Turton, R.; Bailie, R.C.; Whiting, W.B.; Shaeiwitz, J.A. *Analysis, Synthesis, and Design of Chemical Processes*, 3rd ed.; Prentice Hall of India: Hoboken, NJ, USA, 2011.

Disclaimer/Publisher's Note: The statements, opinions and data contained in all publications are solely those of the individual author(s) and contributor(s) and not of MDPI and/or the editor(s). MDPI and/or the editor(s) disclaim responsibility for any injury to people or property resulting from any ideas, methods, instructions or products referred to in the content.